Clays and Clay Minerals, Vol. 68, No. 3:262–272, 2020

CLAY MATERIAL OF AN EOCENE DEPOSIT (KHANGUET RHEOUIS, TUNISIA): IDENTIFICATION USING GEOCHEMICAL AND MINERALOGICAL CHARACTERIZATION

Fathi Allouche[1], Mabrouk Eloussaief[2]*, Sana Ghrab[2], and Nejib Kallel[1]

[1]Laboratoire Géoressources, Matériaux, Environnements et Changements Globaux, LR13ES23, Faculté des Sciences de Sfax, Université de Sfax, BP1171, Sfax 3000, Tunisie

[2]Laboratoire de Recherche 'Eau, Energie et Environnement' (LR3E, code LR99ES35), Ecole Nationale d'Ingénieurs de Sfax, Université de Sfax, BP W, 3038 Sfax, Tunisie

Abstract—Despite the numerous studies on geomaterials in Tunisia, quite a few clay varieties are not yet well defined. In fact no detailed geological, mineralogical, or geochemical characterizations of Tunisian palygorskite deposits have been carried out to date. The purpose of the present work was to study the continental Eocene clay deposit at the southern end of the Tunisian North axis, between Jebel Rheouis and Jebel Boudinar, to determine its potential as a clay reserve. Nine samples were collected from the Cherahil formation representing the lower, middle, and upper levels. The analytical results obtained using several techniques (chemical analysis, X-ray diffraction, specific surface area measurements, Fourier-Transform infrared spectroscopy, scanning electron microscopy) revealed that palygorskite is the dominant clay mineral. Dolomite and quartz are present as associated minerals. Chemical analysis of sample AR9 showed a smaller potassium content compared to other samples. Sample AR9 consists essentially of dolomite associated with palygorskite and quartz. Other samples (AR5, AR6, and AR7) collected from the same Cherahil formation contained palygorskite as the main phyllosilicate mineral (80%). The important reserve of palygorskite was found in the middle of the Cherahil formation. Dolomite and quartz associated with palygorskite reduced the length and crystallinity of the fibrous clay morphology. Analysis by scanning electron microscopy proved that the crystallinity of palygorskite was less in the lower and upper parts of the Cherahil formation. The central palygorskite deposit may be of interest for pharmaceutical (adsorbent drug) and other applications. The two other levels of Cherahil formation are mineralogically heterogeneous and considered economically less important than the middle level, which is rich in palygorskite.

Key Words—Analytical characterization · Crystallinity · Eocene clay deposit · Palygorskite

INTRODUCTION

Since early times, clay has been considered as a noble material due to its abundance, low-cost, efficiency, and eco-friendliness compared to other commercial materials (Mkaouar et al. 2019). Clay minerals are aluminosilicates that are able to exchange cations. The great variety of clay types allows a wide range of uses. The physicochemical properties of clay minerals have been investigated for possible application in many fields including cosmetics (Khiari et al. 2014), pharmacology (Mefteh et al. 2014), environmental application (Ghrab et al. 2014; Ghnainia et al. 2016), ceramics (Jemaï et al. 2017), and fluid refining (Ashraf et al. 2017). The use of clay minerals has evolved with technological developments in such fields as adsorption of terpenic compounds for the synthesis of an insecticidal formulation (Ghrab et al. 2017).

Tunisia has significant reserves of clay materials and several studies have focused on them. For instance, the reserves of kaolin in the Numidian Flysch in Sidi El Bader were investigated by Felhi et al. (2008) and Hafez et al. (2016). Another reserve of smectite in the Coniacian–Santonien Aleg formation was studied by Jarraya et al. (2011).

The Eocene deposit reveals a variety of facies extending from continental deposits in the south to deep marine deposits in the north. This paleogeographic dissimilarity is due to the compressive Triassic halokinetic events along the tectonic fault corridors and folds of the Atlassic domain (Bédir 1995; Boukadi and Bédir 1996). The continental facies are located in two different areas: around Kasserine Island (Burollet 1956; Zouari 1984) and Jeffara Island which were formed at the end of the Upper Cretaceous in the south of Tunisia. The presence of palygorskite deposits, sometimes including sepiolite, has been described by Kadri et al. (1986), Abdeljaoued (1991, 1997), and Jamoussi et al. (2003), who studied the mineralogy and geochemistry of Eocene sequences in many localities around the two islands. The identification of the continental Eocene in central Tunisia was investigated in Jebel Chaambi and the presence of continental facies on the southeastern flank of the Jebel Kebar was revealed (Sassi et al. 1984). Similarly, the continental Eocene facies were detected by Kadri et al. 1986 in the Lessouda and Koumine mountains. The same facies were studied in the Chamsi mountain by Jamousssi et al. (2001) while Abdeljaoued (1983, 1997) determined the continental Bouloufa formation which dated from Lower Eocene in the northern "Chain of Chotts."

The current study aimed to characterize the continental Eocene deposit at the southern end of the northern axis of Tunisia, the Khanguet Rheouis in the Sidi Bouzid region. Significant reserves of clay minerals of Eocene age were observed. This Eocene deposit in Khanguet Rheouis constitutes the Cherahil formation. Cherahil sediments were

* E-mail address of corresponding author: eloussaiefmabrouk@yahoo.fr
DOI: 10.1007/s42860-020-00062-0

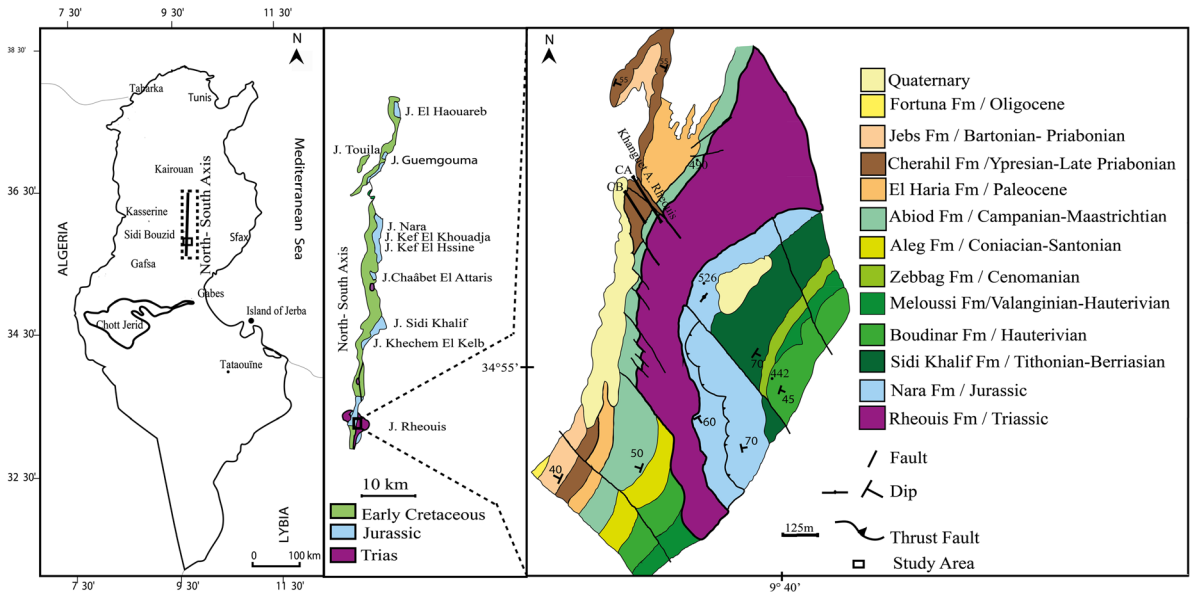

Fig. 1. Location and simplified geological map of Khanguet Rheouis.

deposited on the limestone of the Abiod formation and are surmounted by the Quaternary deposits of the Segui formation.

The Eocene dolomite in central Tunisia has been studied by a number of researchers who explained the occurrence of Eocene dolomite which contains considerable quantities of two fibrous clays (palygorskite and sepiolite). These clays are enriched with other detrital aluminosilicates (illte, smectite, and kaolonite), quartz, and lesser quantities of gypsum and halite. The present study focused on the Eocene dolomite associated with palygorskite in Khanguet Rheouis. The Eocene deposit in the Khaguet Rheouis region of Tunisia has been little studied, but is of fundamental importance for a more complete understanding of the mineralogy of this region.

The mineralogy and geochemical characteristics of the Eocene deposits in Khanguet Rheouis are of great interest. In fact, the homogeneity and the distribution of palygorskite through the dolomitic sequence were evaluated in this study. Finding out whether this clay represents a real economic potential for Tunisia is important. Similarly, can the deposits of primary materials be used widely by the medical and pharmaceutical industries?

GEOLOGICAL SETTING

The outcrops of the Eocene clays in Khanguet Rheouis are located at the junction zone between Jebel Rheouis and Jebel Boudinar (Fig. 1). This area constitutes the southern end of the north–south axis in Tunisia and presents a complex diapiric structure (Abdeljaoued 1991).

The Eocene clays are limited at the southern end of Jebel Rheouis by a narrow strike corridor, marked by two major fractures trending NW–SE. An east–west section of the Khanguet Rheouis region shows that the Eocene clay is limited by two faults: (1) an overlapping inverse fault (FI) trending NNE–SSW in direction; and (2) a strike fault (FD) trending NNW–SSE in direction, disturbed by Triassic evaporite activity (Fig. 1).

The CA and CB sections were made at the joint area of Jebel Meloussi at Khanguet Rheouis. Because the two sections have the same lithostratigraphic succession, a single lithostratigraphic log is presented (Fig. 2). This log reveals the lithostratigraphic succession and details of the sampling from the base to the top. The white chalky limestones and the green clays of the Abiod and El Haria formations were covered by the Cherahil formation of Eocene age. The Cherahil formation consists mainly of clay alternating with dolomitic banks.

MATERIALS AND METHODS

Sampling

In the section studied was the Eocene outcrop represented by the Cherahil formation (75 m). The clay strata alternate with thin dolomite ones. The clay strata become thicker towards the top. The observations of mineral samples from the outcrop show three distinct clay facies: Green clay localized at the base of the geological section, red clay in the middle, and green clay at the top. To determine the mineralogy of the Cherahil samples, nine specimens were analyzed (Fig. 2).

Chemical Analysis

Chemical analysis of the raw samples was performed by dissolving 1 g of dried sample in 25 mL of HNO_3 and 25 mL of HCl. The mixture was evaporated to dryness, then bidistilled water was added to eliminate the remaining traces of acid, and the suspension was filtered with an ashless filter paper (Whatman®) (Eloussaief et al. 2013a). Finally, the chemical composition was determined by atomic adsorption spectrophotometry (ICP-AES). The residue, consisting of insoluble silica (SiO_2), was estimated by gravimetry (Benzina 1990) after calcination at 900°C for 1 h. Loss on ignition (LOI) was considered to be the weight percent difference between samples heated at 100 and 1000°C.

https://doi.org/10.1007/s42860-020-00062-0 Published online by Cambridge University Press

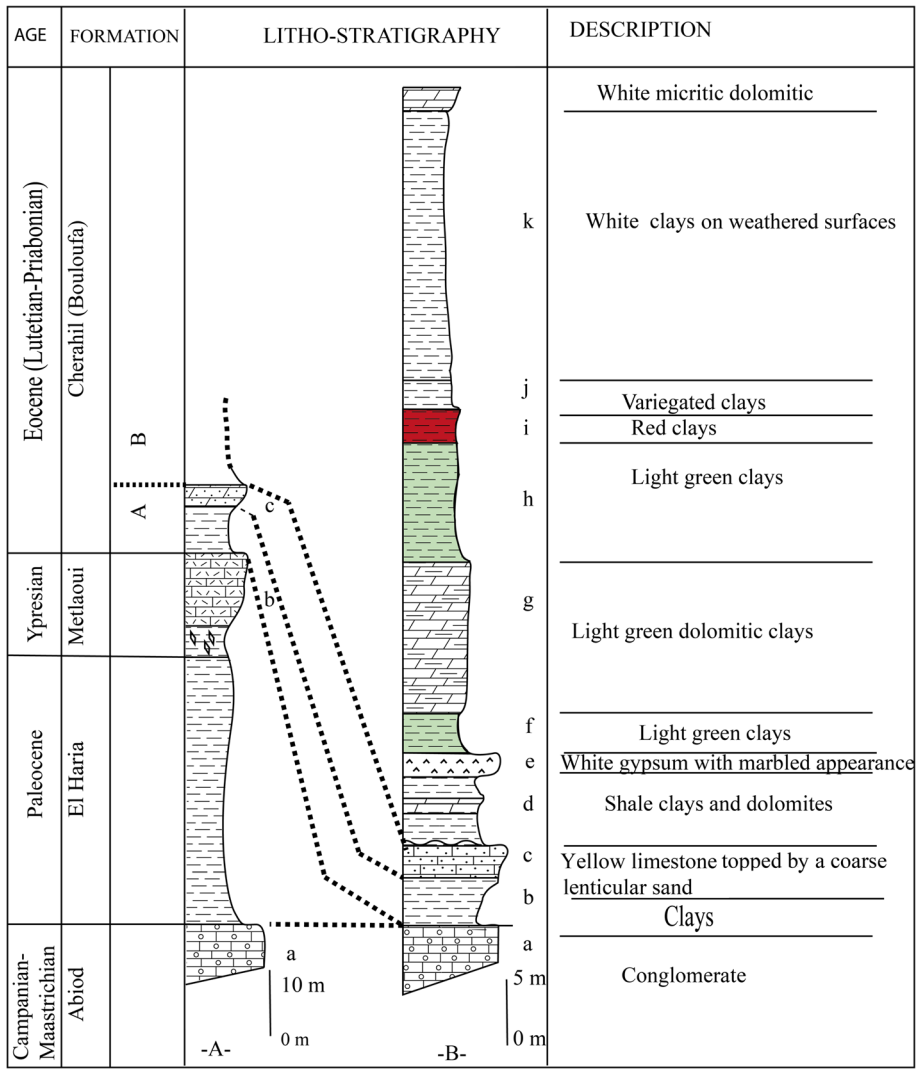

Lithostratigraphic columns of the eastern (A) and western (B) parts of Khaguet Ain Rheouis

Fig. 2. Lithological description of Khanguet Rheouis.

Mineralogical Analysis

X-ray diffraction (XRD) data were obtained using a Philips® X-Pert (Philips Analytical, Almelo, The Netherlands) PW 1710 diffractometer equipped with a CuKα radiation source operating at 40 kV and 40 mA. All XRD data were collected under the same experimental conditions, i.e. over the angular range of 3–45°2θ with an analysis time of 30 min. Natural samples of rock and clay fraction were used to identify the mineralogical associations. The ≤2 μm fraction was separated by sedimentation and centrifugation at 2500 rpm (1540×*g*) for 20 min (Sdiri et al. 2010; Eloussaief et al. 2013b). The diffraction data were analyzed using the X'Pert *HighScore Plus*® software (Martin-Ramos 2004).

Textural Analysis

The textural analysis was performed only for the representative sample AR6 from the Cherahil formation. The specific surface area was determined by the adsorption-desorption isotherms of nitrogen (BET-Specific Surface area and Porosity Analyzer 2020, Micromeritics, Merignac, France).

https://doi.org/10.1007/s42860-020-00062-0 Published online by Cambridge University Press

Table 1 Chemical composition (wt.%) of samples.

	SiO_2	MgO	Al_2O_3	K_2O	Na_2O	Fe_2O_3	CaO	LOI	Total
AR1	28.584	10.598	4.312	0.538	0.15	1.702	16.790	33.76	96.434
AR2	27.692	9.872	3.811	0.534	0.16	1.705	16.683	35.50	95.957
AR3	22.984	11.255	2.663	0.328	0.27	1.184	23.173	35.05	96.907
AR4	31.613	7.916	4.732	0.994	0.11	2.561	15.207	34.67	97.803
AR5	35.353	7.940	6.069	1.105	0.15	3.205	11.46	30.16	95.442
AR6	33.160	7.710	5.800	1.090	0.13	2.98	13.12	33.60	97.690
AR7	31.449	5.907	5.802	2.000	0.11	3.451	13.981	35.40	97.944
AR8	26.507	8.869	4.698	1.016	0.21	2.321	18.135	33.88	95.636
AR9	14.961	12.671	2.517	0.268	1.50	0.734	26.978	36.18	95.809

FTIR Spectroscopy

The Fourier-transform infrared spectrometry (FTIR) was recorded in the 4000–400 cm^{-1} range using a Bruker Equinox 55 spectrometer (Bruker, Kennewick, Washington, USA). The samples were prepared using the KBr pellet method. All the samples were studied under the same hydration conditions, kept over H_2SO_4 solutions (relative humidity RH = 45%). The clay mixtures and dried KBr (ratio 1:200) were subjected to a pressure of 785 MPa. Statistical treatment of the data was carried out using the *SPSS 10.0* program.

Morphology Analysis

The morphology of the raw sample was examined using scanning electron microscopy (SEM - Philips® 30 SEM, Philips Electron Optics, Ottoway, Australia) and microanalysis was conducted by associated energy-dispersive X-ray spectroscopy (EDX). The raw sample fragments were coated with gold prior to analysis (Eloussaief et al. 2011). The SEM images were obtained using a secondary electron detector.

RESULTS AND DISCUSSION

Chemical Analysis

Chemical analysis of the Cherahil formation samples (Table 1) showed that the clay fractions have significant SiO_2 and Al_2O_3 contents, ranging between 15 and 35.3 wt.% for SiO_2 and between 2.5 and 6 wt.% for Al_2O_3. All of the samples displayed a large MgO content ranging from 5 to 12 wt.%, except for the middle samples. The large MgO content is related to dolomite (Zhu et al. 2016). Further, Mg^{2+} may be incorporated in the octahedral sheet of phyllosilicates (Tlili et al. 2010). The Fe_2O_3 content varied from 0.7 to 3.45 wt.%. The clays are impure and heterogeneous. The iron deficiency is associated with the reduced depositional environment. The remaining Fe is the iron oxide which was already obtained from the clay.

On the other hand, the alkaline cation contents of the samples revealed that the amounts of K_2O and Na_2O do not vary significantly. The small K_2O contents are due to the trace amounts of potassic clay minerals, probably illite (Felhi et al. 2008). The AR_2 sample, located below the gypsum layer, is an exception as it contains 0.11 wt.% of Na_2O. This richness in Na_2O is associated with the alteration of the gypsum member. The largest LOI, determined by calcination, was attributed to the evaporation of physically bound water, the dehydroxylation of clay minerals, and the decomposition of carbonate minerals.

A negative correlation was observed between Al and Mg (Fig. 3), which means that Al belongs to clay minerals and Mg belongs mostly to dolomite in the lower part of the Cherahil formation. Al and Mg belong to both the clay and non-clay fractions of the collected samples. Another negative correlation was found between Al and Mg, indicating that Ca belongs mostly to dolomite. The calcium does not belong to the fibrous structures. It can be derived from the impurities associated with the clay minerals. The curves show correlations between Al_2O_3/Na_2O and Al_2O_3/K_2O. Potassium and sodium, therefore, are incorporated into the interlayer space of the clay minerals and the positive correlation with Al_2O/Fe_2O_3 confirms that Fe occupies the octahedral site of the clay mineral. It may also be present in the form of Fe (oxyhydr)oxide.

Mineralogical Analysis

The XRD pattern of sample AR6 was considered to be representative because that sample contained a large percentage of palygorskite (Fig. 4) as indicated by the reflections at 10 Å (Zha et al. 2013). The palygorskite is associated with dolomite and quartz which were detected by the (104) reflection at 2.88 Å and the (101) reflection at 3.34 Å.

The mineralogical compositions of all the samples (Table 2) show that the base of the Cherahil formation is moderately rich in palygorskite associated with dolomite. The findings obtained were correlated with the chemical analysis which confirmed the presence of carbonate and magnesium elements. Toward the middle level of the Cherahil formation, the dominant palygorskite is related to a decrease in carbonate and magnesium in samples AR5, AR6, and AR7.

For some levels, the palygorskite was associated more with dolomite and siliceous crystals which reach up to 80 wt.%. Palygorskite alternates with dolomite levels, especially toward the lowest and upper most parts of the Cherahil formation. Further, the association palygorskite/dolomite is a result of the trapped clay between the dolomite blocks.

https://doi.org/10.1007/s42860-020-00062-0 Published online by Cambridge University Press

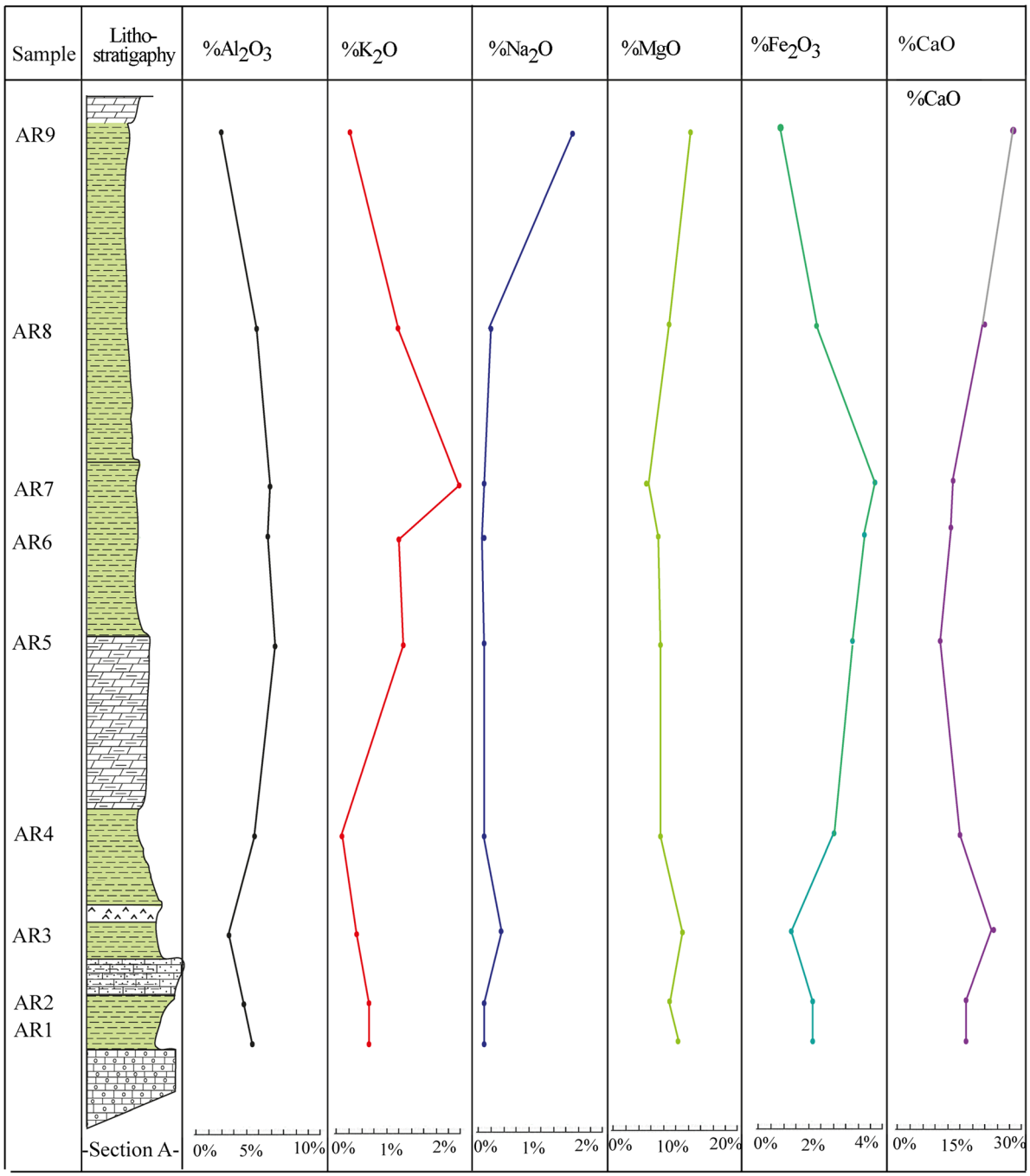

Fig. 3. Chemical composition correlated with the locations of the samples collected.

Overall, the results of mineralogical analyses of the samples collected from the Cherahil formation show a lateral homogeneity of the Eocene deposit clay from east (CA) to west (CB) (Fig. 5).

Textural Analysis

The nitrogen adsorption-desorption isotherms of the representative sample AR6 (Fig. 6) together with the BET specific surface area (Table 3) were classified as type III behavior by the classification of Brunauer, Deming, Deming, and Teller (BDDT) (Brunauer et al. 1940). The curves of AR6 had different hysteresis loops compared with those of smectite (Park et al. 2011; Affouri et al. 2015). The saturation of AR6 by N_2 was not completed. This analysis revealed that the AR6 structure consists of smaller fibers which build up bundles of developed pore channels.

https://doi.org/10.1007/s42860-020-00062-0 Published online by Cambridge University Press

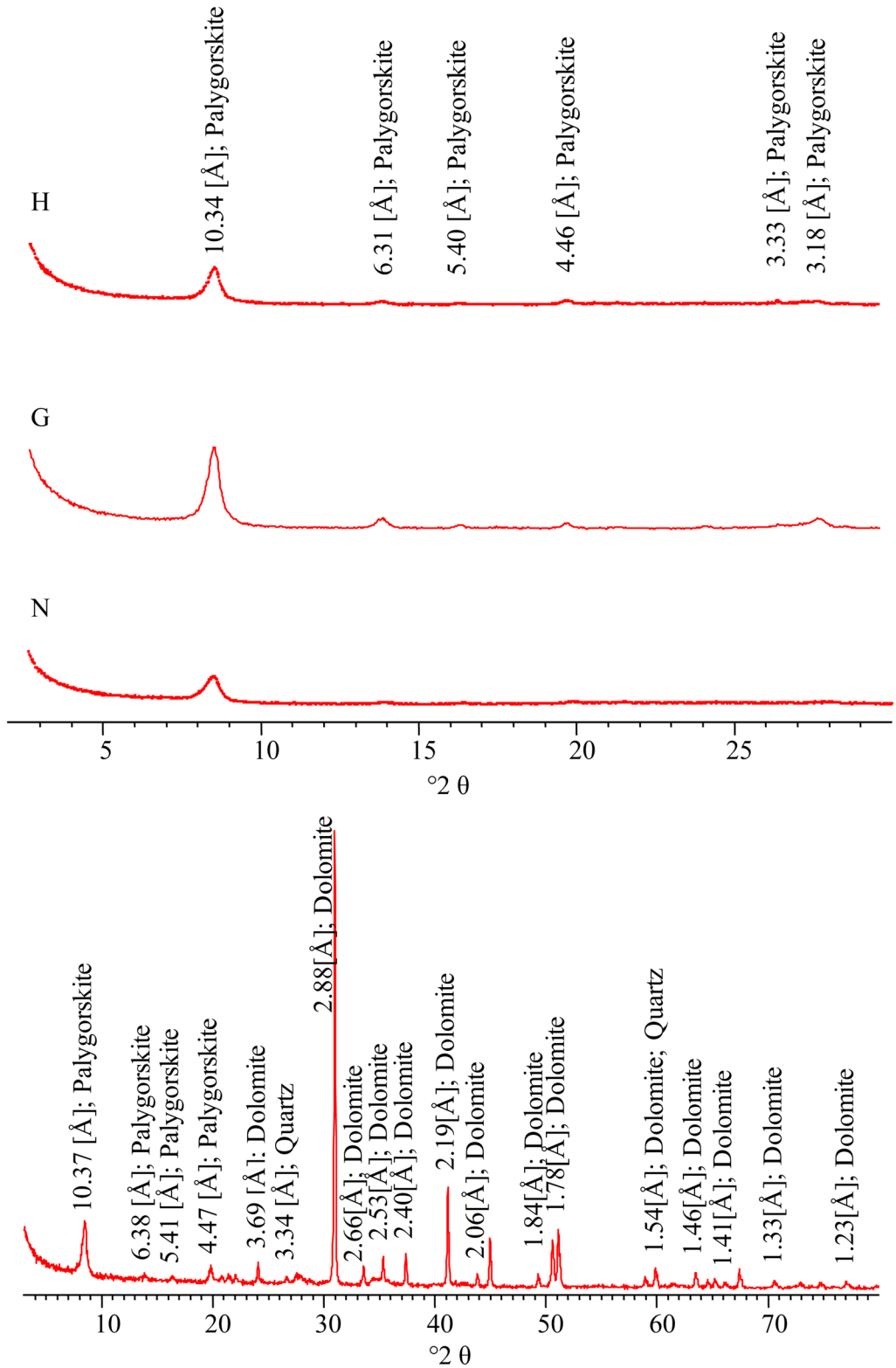

Fig. 4. XRD patterns of total rock (TR) and oriented aggregates: normal (N), glycolated (G) and heated, at 550°C (H), of representative sample (AR6)

https://doi.org/10.1007/s42860-020-00062-0 Published online by Cambridge University Press

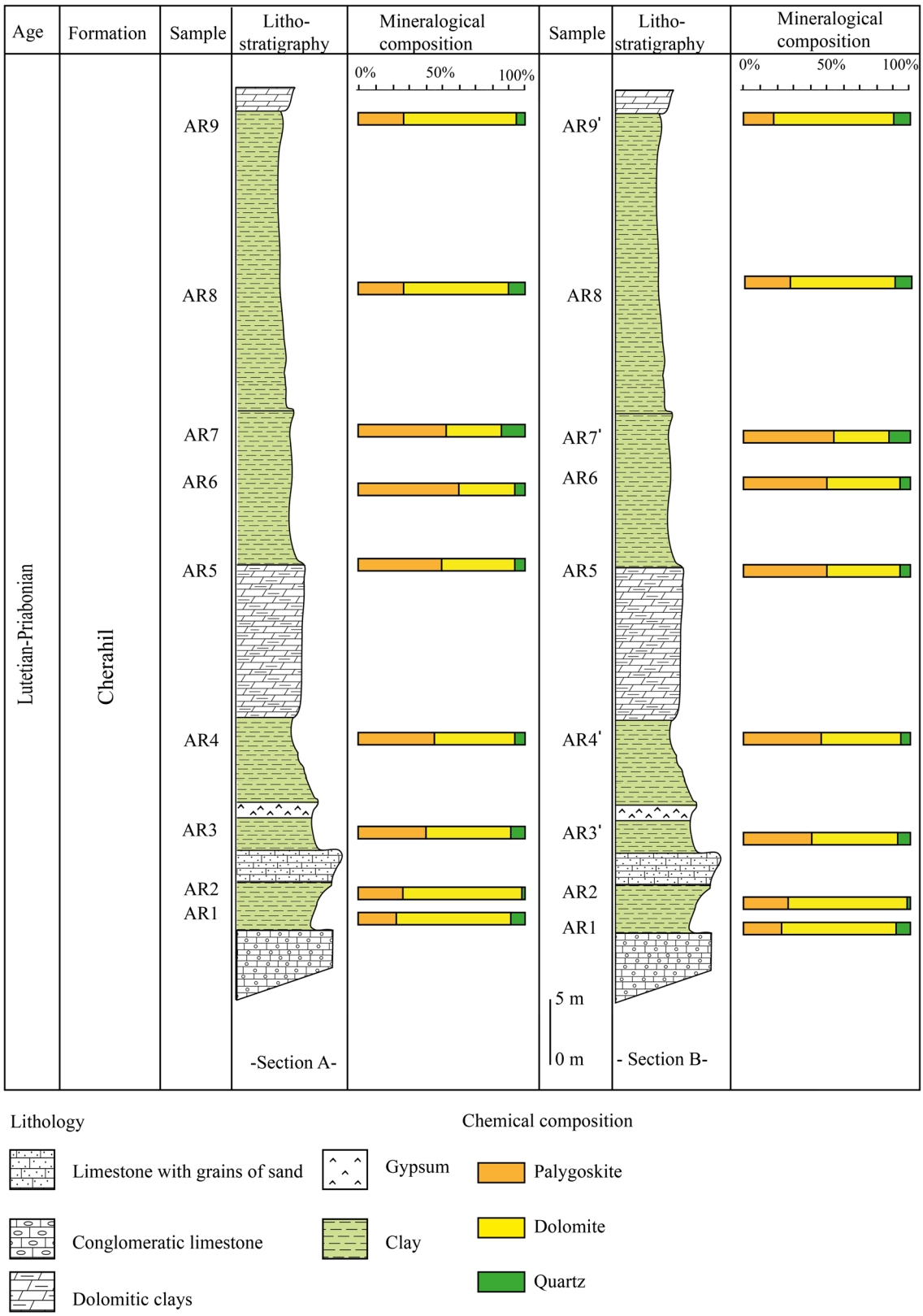

Fig. 5. Mineralogical variation of Cherahil formation samples in the CA and CB sections.

https://doi.org/10.1007/s42860-020-00062-0 Published online by Cambridge University Press

Table 2 Mineralogical composition of samples.

	Total rock mineralogy (wt.%)		
	Clay minerals	Non-clay minerals	
	Palygorskite	Dolomite	Quartz
AR1	25.32	71.33	3.35
AR2	27.06	68.30	4.64
AR3	40.04	56.90	3.06
AR4	45.91	52.00	2.09
AR5	65.00	32.31	2.69
AR6	80.38	18.56	1.06
AR7	68.55	28.38	3.07
AR8	28.64	67.36	4.00
AR9	26.32	70.20	3.48
AR3'	40.04	56.90	3.06
AR4'	45.91	52.00	2.09
AR7'	53.55	41.31	5.14
AR9'	18.83	77.15	4.02

The main textural constants are summarized in Table 3. The BET specific surface area was estimated to be 61 m^2/g.

FTIR Spectroscopy

The FTIR spectra revealed important peaks (Fig. 7). Firstly, the band at 3543 cm^{-1} was assigned to coordinated water; a contribution of the OH-stretching mode in Al–Mg–OH, Fe–Mg–OH, and Fe–OH groups was also considered. The peak observed in sample AR6 agreed well with this observation because it is rich in magnesium. The lowest wavenumbers occurred between 1200 and 500 cm^{-1}, characteristic of Si–O groups in the tetrahedral sheet. Frost et al. (2001) assigned the absorption bands found between 990 and 615 cm^{-1} to M–OH deformation. For the sample studied here, the peak located at 1190 cm^{-1} was regarded as characteristic of palygorskite.

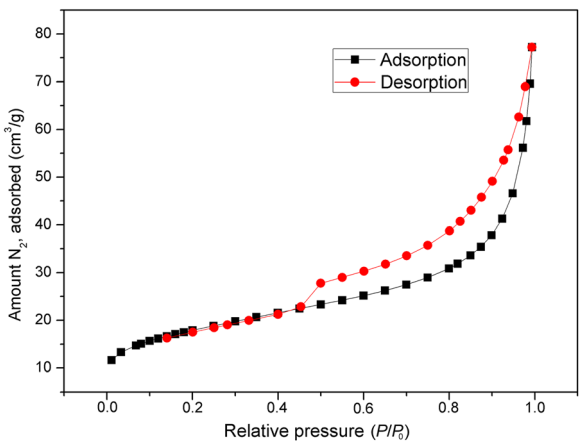

Fig. 6. N_2 adsorption/desorption isotherms of sample AR6 from the Cherahil formation.

Table 3 Specific surface area (S_{BET}), pore volume (V_p), and pore diameter (P_s) of representative sample AR6.

	S_{BET} (m^2/g)	V_p (cm^3/g)	(P_s) (Å)
AR6	61	0.144	74.344

The presence of small quantities of impurities can easily be detected in the FTIR spectra (Fig. 7). Calcite or dolomite was detected in the AR6 sample by the characteristic band at 1433 cm^{-1} and a shoulder at 876 cm^{-1}. As for quartz, it was detected at 728 and 615 cm^{-1}.

Morphology

Representative samples of the basal level (AR1, AR3), middle level (AR6), and top level (AR7) were chosen for SEM analysis (Fig. 8); the results reflected the compositions determined by XRD (Table 4).

The SEM image of the AR1 sample (Fig. 8) showed that the bottom of the Cherahil formation consists of an abundance of well developed rhombohedral crystals which correspond to dolomite. The presence of dolomite in AR3 was confirmed by EDX analysis. This analysis revealed a Mg content of 9% and average contents of Al and K of 4 and 0.4%. All the samples showed a smaller K content. These results are in total agreement with the chemical and mineralogical analyses.

The AR6 sample was made up of rod-like particles of variable thicknesses and lengths packed densely in a randomly oriented network (Xu et al. 2014). The presence of palygorskite increases toward the middle of the Cherahil formation. Palygorskite is associated with dolomite crystals along this formation (AR3), indicating that the dolomitization process began during early diagenesis. Moreover, the mineral impurities reduce the size and crystallinity of the fibrous clay from the clay deposits in the lower part of the Cherahil formation. The characteristic morphology correlates with some other studies including those of Yuan et al. (2007) and Qiu et al. (2015). The presence of palygorskite was confirmed by a Mg content of between 6.3 and 9.72%.

On the other hand, the density of crystallized palygorskite in sample AR7 was low. The rod-like particles were in parallel orientation and packed densely, with impurities. Palygorskite exhibits that same fibrous texture and appears most commonly as chaotic arrangements of short fibers, i.e. of <2 μm. The crystal lattice has the structure of a hollow brick the cavities of which are filled with water (Zhang et al. 2015).

In terms of other palygorskites from Saudi Arabia, New Zealand, Senegal, and the United Arab Emirates described in previous studies (Cagatay 1990; Soong 1992; Garcia-Romero et al. 2007; Draidia et al. 2016), the geochemical and textural results observed here indicate that the genesis of this type of clay was probably by direct precipitation from Ca-, Mg-, Al-, Fe-, and Si-rich solutions or recrystallization of smectite. The morphology

https://doi.org/10.1007/s42860-020-00062-0 Published online by Cambridge University Press

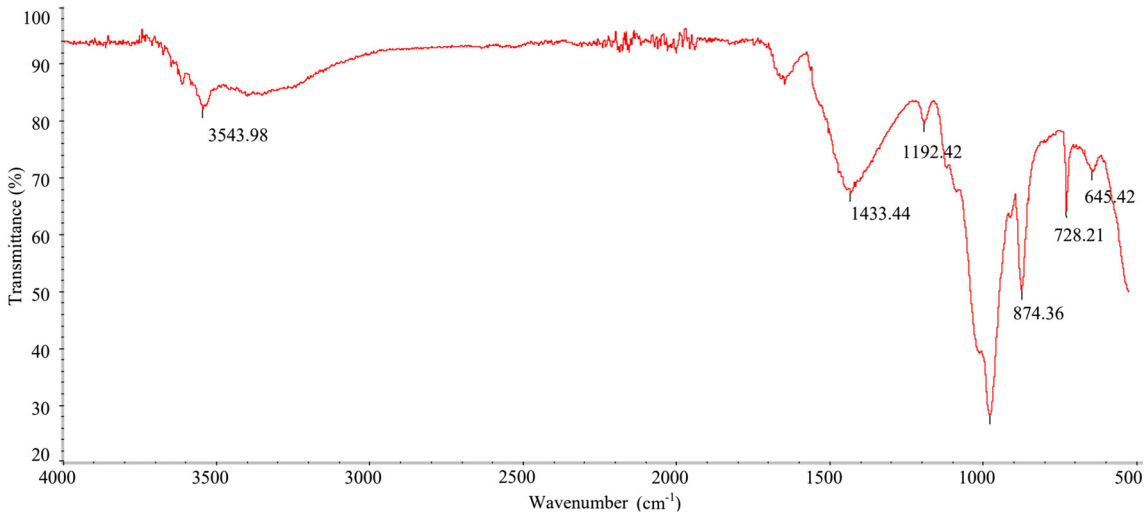

Fig. 7. FTIR spectra of representative sample AR6.

of palygorskite resembles that of a 2:1 fibrous phyllosilicate with isolated fibers and associated with dolomite and small quantities of quartz (Cagatay 1990; Soong 1992; Garcia-Romero et al. 2007; Draidia et al. 2016). The palygorskite contains mainly Mg, Al, Si, and Fe with a significant Mg content. The Mg concentrations combined with the presence of dolomite were sufficient to generate the palygorskite material.

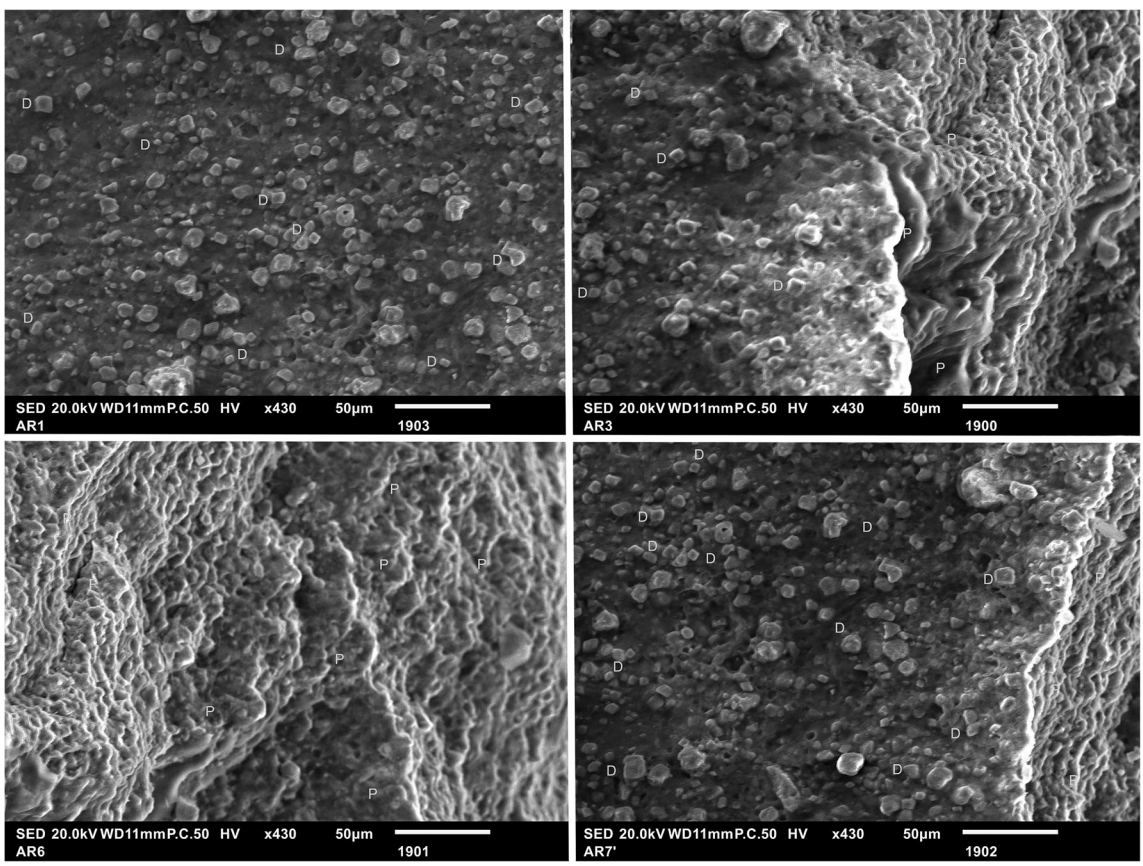

Fig. 8. SEM images (D: Dolomite, P: Palygorskite) showing the morphology of the samples collected from the Cherahil formation.

https://doi.org/10.1007/s42860-020-00062-0 Published online by Cambridge University Press

Table 4 EDX microanalyses of samples AR1, AR3, AR6, and AR7′.

Atomic (%)	AR1	AR3	AR6	AR7′
Si	26.11	16.38	27.95	29.3
Al	8.79	3.83	4.98	8.26
Mg	3.97	9.72	7.56	6.45
Ca	5.64	8.8	7.62	1.94
K	1.28	0.42	1.06	2.53
O	47.37	23.11	19.93	46.62
Na	0	19.77	15.43	0.66
Cl	0	15.87	10.83	0
Fe	0	2.07	4.6	4.2

The formation of deposits of the palygorskite in the present study zone occurred during evaporative oxidizing conditions and took place during Eocene, Oligocene, and Mio-Pliocene times (Cagatay 1990; Soong 1992; Garcia-Romero et al. 2007; Draidia et al. 2016). The formation of palygorskite required specific conditions such as alkaline pH and large amounts of Mg. The chemical changes were probably due to climatic fluctuations and/or gypsum precipitation. The amount of Mg may have led to the various generations of dolomite and to the appearance of palygorskite.

CONCLUSIONS

The mineralogy and physiochemical characterization of Cherahil-formation material revealed the presence of Mg-rich clay and dolomite crystallization increasing towards the top of the formation. Palygorskite deposits of Eocene age showed a lateral homogeneity in the Cherahil formation from east (CA) and west (CB). This material represents a very important reserve of palygorskite (80%) and should be investigated for use in the pharmaceutical industry, e.g. as a hydrated adsorbent (gel) or a dehydryated adsorbent, and (following slight purification) as an anti-diarrheal product, and in cosmetics products. It could also be a valuable resource in other industries, e.g. in the separation of fluids, in agriculture as a suspended fertilizer, in environmental applications as an adsorbent in photo-catalysis, and also in drilling technologies.

ACKNOWLEDGMENTS

The authors are grateful to Prof. Abdelmajid Dammak for his checking of the English in the manuscript.

Compliance with Ethical Standards

CONFLICT OF INTEREST

We confirm that there are no known conflicts of interest associated with this publication and there has been no significant financial support for this work that could have influenced its outcome.

REFERENCES

Abdeljaoued, S. (1983). Étude sédimentologique et structurale de la partie est de la chaîne nord des Chotts (Tunisie méridionale). *Thèse, Université de Tunis*, 148 pp.

Abdeljaoued, S. (1991). Les dolocrètes et les calcrètes du Paléocène–Éocène, Tunisie méridionale. *Thèse d'État, Université de Tunis, 2*, 242 pp.

Abdeljaoued, S. (1997). Mode de genèse des palygorskites dans la série continentale éocène de Tunisie méridionale. *Notes du Service géologique, Tunisie, 63*, 15–27.

Affouri, A., Eloussaief, M., Kallel, N., & Benzina, M. (2015). Application of Tunisian limestone material for chlorobenzene adsorption: characterization and experimental design. *Arabian Journal of Geoscience, 8*, 11183–11192.

Ashraf, M. A., Hussain, I., Rasheed, R., Iqbal, M., Riaz, M., & Arif, M. S. (2017). Advances in microbe-assisted reclamation of heavy metal contaminated soils over the last decade: a review. *Journal of Environmental Management, 198*, 132–143.

Bédir, M. (1995). Mécanismes géodynamiques des bassins associés aux couloirs de coulissement de la marge Atlasique de la Tunisie. *Séismo-stratigraphie, séismo-tectonique et implications pétrolières, Thèse d'État, université de Tunis, 2*, 407.

Benzina, M. (1990). Kinetic study and thermodynamic of organic adsorption onto local clays, Modelling adsorbant on bed fixed. *Thesis of Doctorat of Physic Sciences*, *Faculty of Sciences of Tunis*, 25.

Boukadi, N., & Bédir, M. (1996). L'halocinèse en Tunisie: contexte tectonique et chronologie des événements, C. R. *Académie des Sciences*. *Paris, série IIa, 322*, 587–594.

Brunauer, S., Deming, L. S., Deming, W. E., & Teller, E. (1940). On a theory of the van der Waals adsorption of gases. *Journal of American Chemical Society, 62*, 1723.

Burollet, P. F. (1956). Contribution à l'étude stratigraphique de la Tunisie centrale. *Annales des Mines et de la Géologie, Tunis, 18*, 1–350.

Cagatay, M. N. (1990). Palygorskite in the Eocene rocks of the dammam dome, Saudi Arabia. *Clays and Clay Minerals, 38*, 299–307.

Draidia, S., El Ouahabi, M., Daoudi, L., Havenith, H. B., & Fagel, N. (2016). Occurrences and genesis of palygorskite/sepiolite and associated minerals in the Barzaman formation, United Arab Emirates. *Clay Minerals, 51*, 763–779.

Eloussaief, M., Bouaziz, S., Kallel, N., & Benzina, M. (2013a). Valorisation of El Haria clay in the removal of arsenic from aqueous solution. *Desalination Water Treatment, 52*, 2220–2224.

Eloussaief, M., Kallel, N., Yaacoubi, A., & Benzina, M. (2011). Mineralogical identification, spectroscopic characterization, and potential environmental use of natural clay materials on chromate removal from aqueous solutions. *Chemical Engineering Journal, 168*, 1024–1031.

Eloussaief, M., Sdiri, A., & Benzina, M. (2013b). Modelling the adsorption of mercury onto natural and aluminium pillared clays. *Environmental Science Pollution Research, 20*, 469–479.

Felhi, M., Tlili, A., Gaied, M. E., & Montacer, M. (2008). Mineralogical study of kaolinitic clays from Sidi El Bader in the far north of Tunisia. *Applied Clay Science, 39*, 208–217.

Frost, R. L., Locos, O. B., Ruan, J., & Kloprogge, J. T. (2001). Near-infrared and mid-infrared spectroscopic study of sepiolites and palygorskites. *Vibrational Spectroscopy, 27*, 1–3.

Garcia-Romero, E., Suarez, M., Santaren, J., & Alvarez, A. (2007). Crystallochemical characterization of the palygorskite and sepiolite from the Allou Kagne deposit, Senegal. *Clays and Clay Minerals, 55*, 606–617.

Ghnainia, L., Eloussaief, M., Zouari, K., & Abbes, C. (2016). Wastewater treatment in petroleum activities: example of "SEWAGE" unit in the BG Tunisia Hannibal plant. *Applied Petrochemical Research, 6*, 155–162.

https://doi.org/10.1007/s42860-020-00062-0 Published online by Cambridge University Press

Ghrab, S., Boujelben, N., Medhioub, M., & Jamoussi, F. (2014). Chromium and nickel removal from industrial wastewater using Tunisian clay. *Desalination Water Treatment, 52*, 2253–2260.

Ghrab, S., Eloussaief, M., Lambert, S., Bouaziz, S., & Benzina, M. (2017). Adsorption of terpenic compounds onto organo-palygorskite. *Environmental Science Pollution Research, 25*, 18251–18261.

Hafez, A. I., Naser, S. G., Ibrahim, H. N., Abou El-magd, W. S. I., & Hashem, A. (2016). Evaluation of kaolin clay as natural material for transformer oil treatment to reduce the impact of ageing on copper strip. *Egyptian Journal of Petroleum, 26*, 533–539.

Jamoussi, F., Abbès, C., Fakhfakh, E., Bédir, M., Kharbachi, S., Soussi, M., Zargouni, F., & López-Galindo, A. (2001). Découverte de l'Éocène continental autour de l'archipel de Kasserine, aux Jebels Rhéouis, Boudinar et Chamsi en Tunisie centro-méridionale: nouvelles implications paléogéographiques. *Comptes Rendus d'académie des Sciences -Série IIA-Earth and Planetary Science, 333*, 329–335.

Jamoussi, F., Bédir, M., Boukadi, N., Kharbachi, S., Zargouni, F., López-Galindo, A., & Paquet, H. (2003). Evolution minéralogique des argiles et contrôle tectono-eustatique des bassins de la marge Tunisienne. *Geoscience, Géomatériaux / Geomaterials, 335*, 175–183.

Jarraya, I., Fourmentin, S., Benzina, M., & Bouaziz, S. (2011). The characterization of prepared organoclay materials (ddma) and gas sorption of chlorobenzene. *The Canadian Journal of Chemical Engineering, 89*, 392–400.

Jemaï, M. B. M., Sdiri, A., Ben Salah, I., Ben Aissa, L., Bouaziz, S., & Duplay, J. (2017). Geological and technological characterization of the Late Jurassic-Early Cretaceous clay deposits (Jebel Ammar, northeastern Tunisia) for ceramic industry. *Journal of African Earth Science, 129*, 282–290.

Kadri, A., Matmati, F., Ben Ayed, N., & Ben Haj Ali, M. (1986). Découverte de l'Éocène inférieur continental au Jebel Lessouda (Tunisie centrale). *Notes du Service géologique*, *Tunisie, 51*, 53–59.

Khiari, I., Mefteh, S., Sánchez-Espejo, R., Cerezo, P., Aguzzi, C., López-Galindo, A., Jamoussi, F., & Viseras Iborra, C. (2014). Study of traditional Tunisian medina clays used in therapeutic and cosmetic mud-packs. *Applied Clay Science, 101*, 141–148.

Martín-Ramos, J. (2004) D. X-Powder, a software package for powder X-ray diffraction analysis. Legal Deposit G.R.1001/04, http://www.xpowder.com.

Mefteh, S., Khiyari, I., Sanchez-Espejo, R., Aguzzi, C., Lopez Galindo, A., Jamoussi, F., & Viseras, C. (2014). Characterisation of Tunisian layered clay materials to be used in semisolid health care products. *Materials Technology Journal, 29*, B88–B95.

Mkaouara, S., Maherzib, W., Pizette, P., Zaitan, H., & Benzina, M. (2019). A comparative study of natural Tunisian clay types in the formulation of compacted earth blocks. *Journal of African Earth Science, 160*, 103620.

Park, Y., Godwin, A., Ayoko, & Frost, R. L. (2011). Characterization of organoclays and adsorption of p-nitrophenol: Environmental application. *Journal of Colloid and Interface Science, 360*, 440–456.

Qiu, G., Xie, Q., Liu, H., Chen, T., Xie, J., & Li, H. (2015). Removal of Cu (II) from aqueous solutions using dolomite–palygorskite clay: Performance and mechanisms. *Applied Clay Science, 118*, 107–115.

Sassi, S., Triat, J.-M., Truc, G., & Millot, G. (1984). Découverte de l'Éocène continental en Tunisie centrale: la formation du Djebel Gharbi et ses encroûtements carbonatés, C. R. *Académie des Sciences*. *Paris, série II, 299*, 357–364.

Sdiri, A., Higashi, T., Hatta, T., Jamoussi, F., & Norio, T. (2010). Mineralogical and spectroscopic characterization, and potential environmental use of limestone from the Abiod formation, Tunisia. *Environmental Earth Science, 61*, 1275–1287.

Soong, R. (1992). Palygorskite occurrence in northwest Nelson, South Island, New Zealand. *Journal of Geology and Geophysics, 35*, 325–330.

Tlili, A., Felhi, M., & Montacer, M. (2010). Origin and depositional environment of palygorskite and sepiolite from the Ypresian phosphatic series, Southwestern Tunisia. *Clays and Clay Minerals, 58*, 573–581.

Xu, J., Wang, W., & Wang, A. (2014). Effect of squeeze, homogenization, and freezing treatments on particle diameter and rheological properties of palygorskite. *Advanced PowderTechnology, 25*, 968–977.

Yuan, X., Li, C., Guan, G., Liu, X., Xiao, Y., & Zhang, D. (2007). Synthesis and characterization of polyethylene terephthalate/attapulgite nanocomposites. *Journal of Applied Polymer Science, 103*, 1279–1286.

Zha, F., Huang, W., Wang, J., Chang, J., Ding, J., & Ma, J. (2013). Kinetic and thermodynamic aspects of arsenate adsorption on aluminum oxide modified palygorskite nanocomposites. *Chemical Engineering Journal, 215–216*, 579–585.

Zhang, Y., Wang, W., Zhang, J., Liu, P., & Wang, A. (2015). Comparative study about adsorption of natural palygorskite for methylene blue. *Chemical Engineering Journal, 262*, 390–398.

Zhu, Y., Chen, T., Liu, H., Xu, B., & Xie, J. (2016). Kinetics and thermodynamics of Eu(III) and U(VI) adsorption onto palygorskite. *Journal of Molecular Liquids, 219*, 272–278.

Zouari, H. (1984). Étude structurale du Jebel Chaambi (Tunisie centrale) Relation entre la minéralisation et la structure. Thèse 3e cycle, *Université de Franche-Comté, Besançon*, 93.

(Received 25 April 2019; revised 8 January 2020; AE: Warren D. Huff)